Journal of Physical Chemistry & Biophysics

Nikolopoulos et al., J Phys Chem Biophys 2014, 4:6
DOI: 10.4172/2161-0398.1000168

Research Article Open Access

Hurst Exponent Analysis of Indoor Radon Profiles of Greek Apartment Dwellings

Dimitrios Nikolopoulos[1]*, Ermioni Petraki[2], Nikolaos Temenos[1], Sofia Kottou[3], Dionysios Koulougliotis[4] and Panayotis H Yannakopoulos[1]

[1]*TEI of Piraeus, Department of Electronic Computer Systems Engineering, Petrou Ralli & Thivon 250, GR-12244 Aigaleo, Greece*
[2]*Brunel University, Department of Engineering and Design, Kingston Lane, Uxbridge, Middlesex UB8 3PH, London, UK*
[3]*University of Athens, Medical School, Department of Medical Physics, Mikras Asias 75, GR-11527 Athens, Greece*
[4]*Technological Educational Institute (TEI) of Ionian Islands, Department of Environmental Technology, Neo Ktirio, Panagoula 29100, Zakynthos, Greece*

Abstract

Radon and progeny (^{218}Po, ^{214}Pb, ^{214}Bi and ^{214}Po) are important indoor radioactive air pollutants with impact to humans. Radon is an inert gas that enters buildings from outdoor air, water and soil, especially via gaps around pipes and cables and through cracks in floors. Indoors, radon progeny remain free, or attach to indoor aerosols dust and water droplets. Hence, inhalable indoor radioactive mixtures are created which enter human lungs and irradiate tissues. The radiation exposure depends on several parameters some of which are the building characteristics, local geology, breathing rate and others.

This work aimed to estimate Hurst exponents (H) of time-evolving radon signals of Greek apartment dwellings. The signals were collected with Alpha Guard Pro and include at least 24 hours of measurements in each dwelling. Hurst exponents were calculated by the R/S method through sliding on overlapping windows and lumping on non-overlapping sequential windows. The scope was to identify whether radon dynamics are governed by persistent, anti-persistent behavior or if these are uncorrelated.

Most signals presented significant long-memory segments with important persistent sub- segments.

Keywords: Radon (^{222}Rn); Antipersistency; H- values; Hurst exponents

Introduction

Radon (^{222}Rn) is a naturally occurring radioactive gas generated by the decay of the naturally occurring ^{238}U series [1,2]. Radon is directly produced by the decay of radium (^{226}Ra) which is present in soil, rocks, building materials, underground and surface waters [1,3]. After generation it may dissolve in soil's pores and fluid. Thereafter, it migrates near or far through diffusion or convection and dilutes in atmosphere, surface and groundwater. Radon also dilutes into the atmosphere through release from its aqueous phase [1].

Radon and its progeny are the most significant natural sources of radiation exposure to the general population [3] contributing to about half of the total effective dose delivered to humans from all sources of ionizing radiation. The exposure is mainly delivered in domestic environments since the largest period of human lifetime is spent indoors. Therefore, the measurement and limitation of radon concentration of buildings are important [4].

Moreover, radon has been considered as an additional factor of radiation burden in stomach mainly due to water consumption [5,6]. Various organizations such as WHO, US-EPA and UNSCEAR [3,5,7] refer to this additional burden which can be estimated by measurements of radon concentrations in waters. Regarding Europe the maximum concentration values for radon are proposed by the European Commission [8]. Human exposure to high concentrations of radon and progeny has been correlated to lung cancer incidence [9,10]. For this reason, radon is considered to be a natural carcinogen of great importance.

The typical radon concentrations outdoors are low [3]. However, indoor radon may accumulate at significant levels. Radon accumulation depends on the radioactive properties of the underlying soil and rock, the building structure and the various ways of indoor ventilation and heating [1,3]. Radon in water contributes as well [11,12] and sometimes significantly [13].

During the last few years, several radon time-series were collected from Greek apartment dwellings. The aim of this work was to estimate Hurst exponents (H) of some of these radon time-series. One hundred twenty five radon signals were collected with Alpha Guard Pro and included, at least, one day active measurements in ten minutes cycles. Hurst exponents were calculated by the Rescaled Range (R/S) method. The scope was to identify whether indoor radon is governed by long-memory dynamics namely if persistent, anti-persistent traces can be identified or if the behavior is random, viz. the signals were uncorrelated. R/S method was applied through sliding on overlapping windows and lumping on non-overlapping sequential windows.

Materials and Methods

Hurst exponent

Hurst exponent (H) is a mathematical quantity which can detect long-range dependencies in time-series [14,15]. It can estimate the temporal smoothness of time-series and can search if the related phenomenon is a temporal fractal [16]. Hurst exponent was conceptualized for hydrology [14,15]. It has been employed however

***Corresponding author:** Dimitrios Nikolopoulos, TEI of Piraeus, Department of Electronic Computer Systems Engineering, Petrou Ralli & Thivon 250, GR-12244 Aigaleo, Greece, Tel: +0030-210-5381110; Fax: +0030-210-5381436; E-mail: dniko@teipir.gr; NikolopoulosDimitrios@gmail.com

Received: November 07, 2014; **Accepted:** December 10, 2014; **Published:** December 28, 2014

Citation: Nikolopoulos D, Petraki E, Temenos N, Kottou S, Koulougliotis D, et al (2014) Hurst Exponent Analysis of Indoor Radon Profiles of Greek Apartment Dwellings. J Phys Chem Biophys 4: 168. doi:10.4172/2161-0398.1000168

in other research topics as well, for example, traffic traces [17], plasma turbulence [18], ULF geomagnetic fields [19,20], climatic dynamics [21], pre-epileptic seizures [16], astronomy and astrophysics [22] and economy [23]. H-values between $0.5 < H < 1$ manifest long-term positive autocorrelation in time-series. This means that a high present value will be, possibly, followed by a high future value and this tendency will last for long future time-periods (persistency) [24-27]. *H* - values between $0 < H < 0.5$ indicate time- series with long-term switching between high and low values. Namely, a high present value will be, possibly, followed by a low future value, whereas the next future value will be high and this switching will last long into the future (antipersistency) [24-27]. $H = 0.5$ implies completely uncorrelated time-series.

Rescaled Range Analysis (R/S)

Hurst exponents were estimated through the method of Rescaled Range (R/S) [16] or as frequently referred, R/S analysis. The R/S analysis was introduced by Hurst [14] and attempts to find patterns that might repeat in the future. The method employs two variables, the range, *R* and the standard deviation, *S*, of the data. According to the R/S method, a natural record in time, *X(N) = x(1), x(2),.., x(N),* is transformed into a new variable *y(n,N)* in a certain time period *N(N=1,2,…,N)* from the average, $\langle x \rangle_N = \frac{1}{N}\sum_{i=1}^{N} x(n)$, over a period of *N* time units [14]. *y(n,N)* is called accumulated departure of the natural record in time [14]. The transformation follows the formula:

$$y(n\ N) = \sum_{i=1}^{n} \left(x(i) - \langle x \rangle_N \right) \quad (1)$$

The rescaled range is calculated from (2) [14,16,28] :

$$R/S = \frac{R(n)}{S(n)} \quad (2)$$

The range *R(n)* in (2) is defined as the distance between the minimum and maximum value of *y(n,N)* by :

$$R(n) = \max_{1 \le n \le N} y(n\ N) - \min_{1 \le n \le N} y(n\ N) \quad (3)$$

The standard deviation *S(n)* in (2) is calculated by :

$$S(n) = \sqrt{\frac{1}{N}\left(x(n) - \langle x \rangle_N \right)^2} \quad (4)$$

R/S is expected to show a power-law dependence on the bin size *n*

$$\frac{R(n)}{S(n)} = C \cdot n^H \quad (5)$$

where *H* is the Hurst exponent and *C* is a proportionality constant.

The log transformation of the last equation is a linear relation (6),

$$\log\left(\frac{R(n)}{S(n)} \right) = \log(c) + H \cdot \log(n) \quad (6)$$

from which exponent *H* can be estimated as the slope of the best line fit.

Results

Figure 1 represents a noteworthy case of indoor radon time-series which evolved within approximately two days (47 hours). The corresponding dwelling (D1) was a basement apartment in Athens region. Radon accumulated continuously up to $8kBqm^{-3}$ and then decreased down to approximately $3kBqm^{-3}$. The recorded concentrations were extremely high and considerably above the upper limit of 400 Bqm^{-3} recommended by EU [8]. Three different conditions were applied for the R/S analysis of this dwelling; namely sliding window analysis of length 8 (Figure1a) and 32 (Figure1b) and lumping analysis of length 32 (Figure1c). It can be observed that large sliding windows (Figure1b) produced finer-less deviating Hurst exponents which were well concentrated around high *H*- bands. It is very important that all *H* - values of Figure1b were well above 0.9. It may be recalled that *H* - values between $0.5 < H < 1$ manifest long-term positive autocorrelation in time-series. This means that high present values will be followed, on the most part, by high future values (persistency) while this tendency will last for numerous future time-periods [24-28]. Therefore, the analysis of Figure1b indicates strong-persistent behaviour. Nevertheless, both the analysis of Figure1a (sliding windows) and the one of Figure1c indicate also the persistency of the signal. Indeed, most of the *H*- values were above 0.7, viz., they were persistent. It is also very significant that almost all values of the Spearman's correlation coefficients were successive ($r^2 > 0.95$), namely they corresponded to a very linear log-log R/S fit.

Figure 2 presents a typical case of radon concentrations often observed in Greek apartment dwellings [29,30]. Measurements in this dwelling (D2) spanned approximately four days. Recorded radon concentrations ranged between 10 Bqm^{-3} and 100 Bqm^{-3}. As in Figure 1, most segments exhibited Hurst exponents between 0.5 and 1 with successive square Spearman's correlation coefficient values above 0.98. This fact indicates that these radon time-series are persistent as well. The *H* - profiles however, deviate more compared to those of Figure 1. Despite this, only few *H* - values are below 0.5. The majority of segments are associated with Hurst exponents above 0.7. It is noticeable that in both Figures, the *H* - profiles do not follow those of radon concentration. Most importantly, this is observable in all sub-Figures, namely the tendency is independent of the selection of the window size. These observations provide strong indications regarding strong long-memory underlying dynamics which govern and drive the radon generating system. It is also interesting that larger size of sliding windows, produce also less deviating *H* - values, as in Figure1b. It should be noted however that the analysis should not exceed certain window sizes. For example, the 32 bin window size corresponds to 320 min (32x10min) analysis time. This is the power two window size closest to five hours. Larger windows would render analysis of larger time-windows and this will tend to smooth the *H* - values near large-deviating signal areas, such as peaks and downturns. It should be noted as well, that lumping generates *H* - histograms rather than *H* - profiles. For certain types of long-memory analysis, lumping is considered favorable [28,29,31] mainly because lumping renders to non-overlapping signal's areas. This fact is advantageous for low-deviating segments of the time-series.

Two more interesting results (dwellings D3 and D4) are shown in Figure 3. All Figures correspond to sliding window R/S analysis of window size 32 and window step 1. Hurst exponent profiles of both sub-Figures show analogous patterns which are similar to those of Figures 1b and 2b under identical conditions (window size 32, window step 1). These Figures provide further evidence of the underlying long-memory radon dynamics. Once again, the profiles of Hurst exponents are different from those of the variation of radon concentration. This is of extreme importance, especially if it is considered that radon concentration variations are affected by various factors and, most importantly, in a multivariate manner [32]. Radon concentrations of Figure3 are below the EU upper action limit for radon concentration, viz. below 400 $Bq.m^{-3}$. Both radon profiles are also typical for Greek apartment dwellings [30]. Figure 4 presents collectively the results from the R/S analysis of all investigated dwellings. Hurst exponents were calculated through sliding window analysis of window size 8 (Figure 4a), 16 (Figure 4b) and 32 (Figure 4c). As aforementioned, larger size of sliding windows produces less-deviating Hurst exponents. It is important that for all

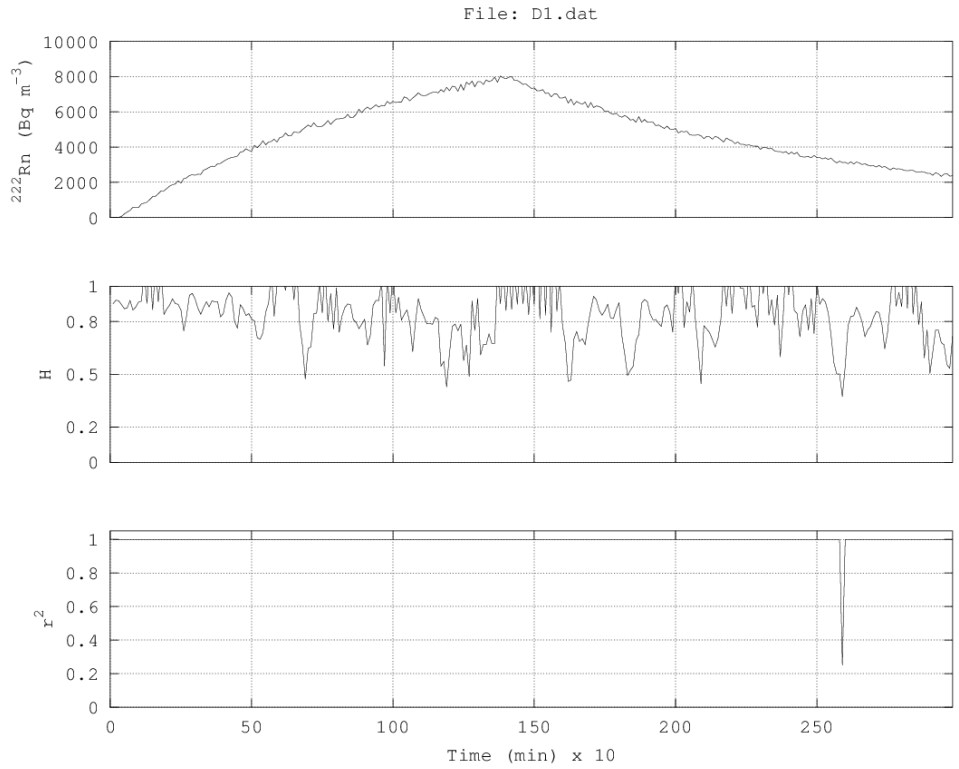

(a)

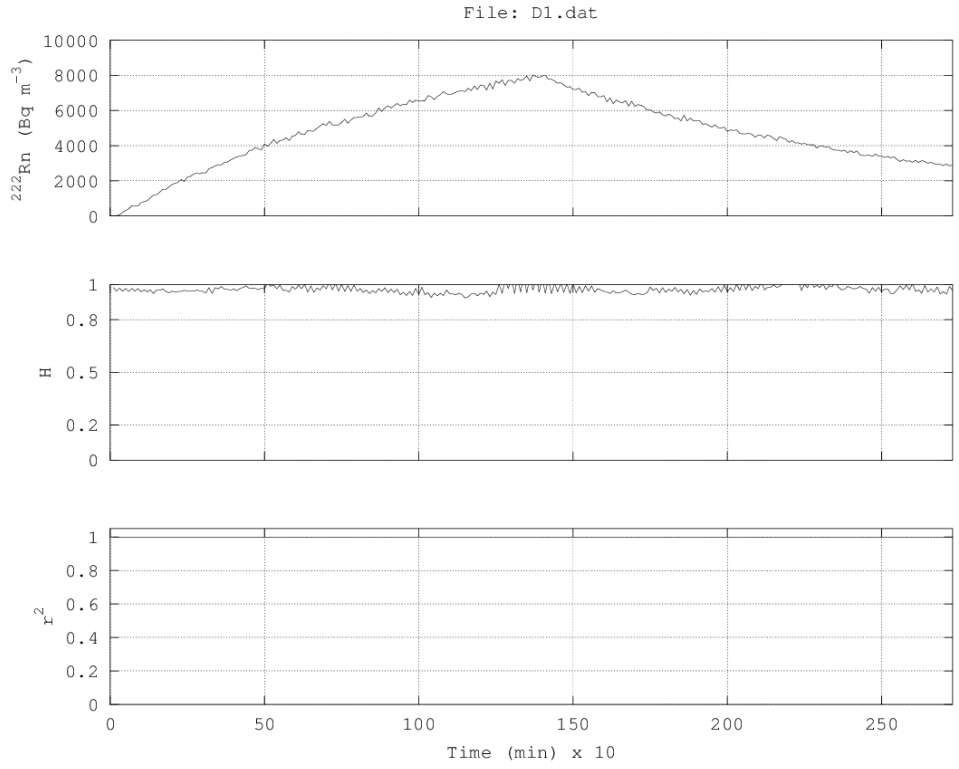

(b)

Figure 1: Flow chart depicting steps involved in MD simulation of a protein.

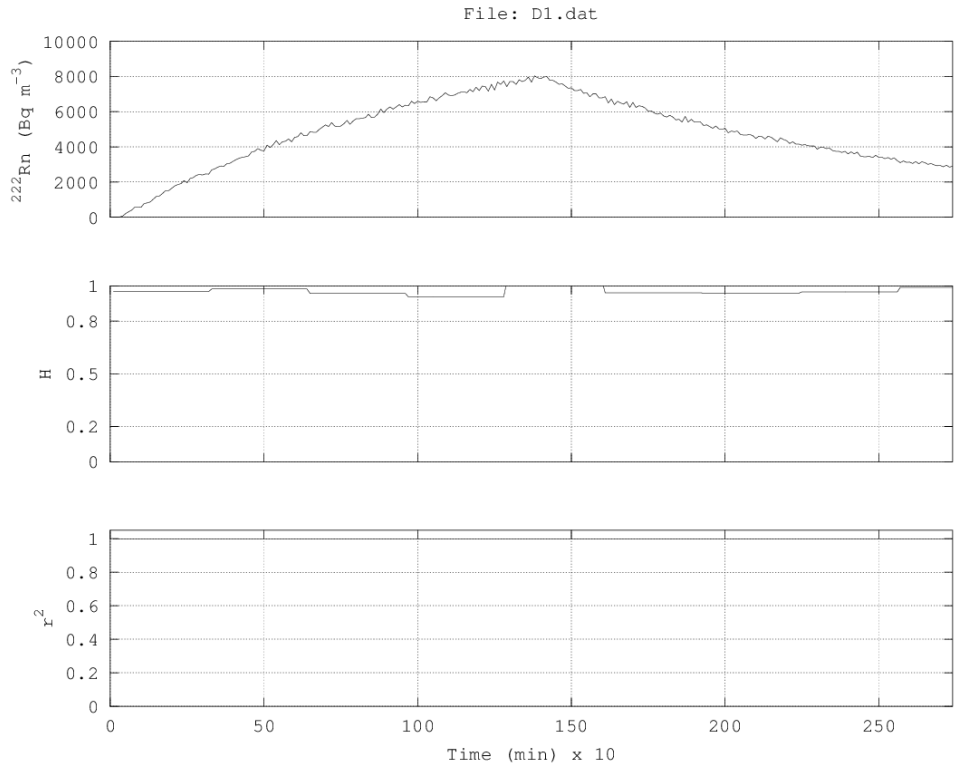

(c)

Figure 1: Radon concentration and Hurst exponent evolution in dwelling D1. In all Figureures, the top sub-Figureure is the evolution of radon concentration, the middle sub-Figureure is the evolution of Hurst exponent and the bottom sub-Figureure is the evolution of the square of the linear correlation coefficient. R/S analysis: (a) sliding-window of length 8, step 1; (b) sliding-window of length 32, step 1; (c) lumping of window-length 32.

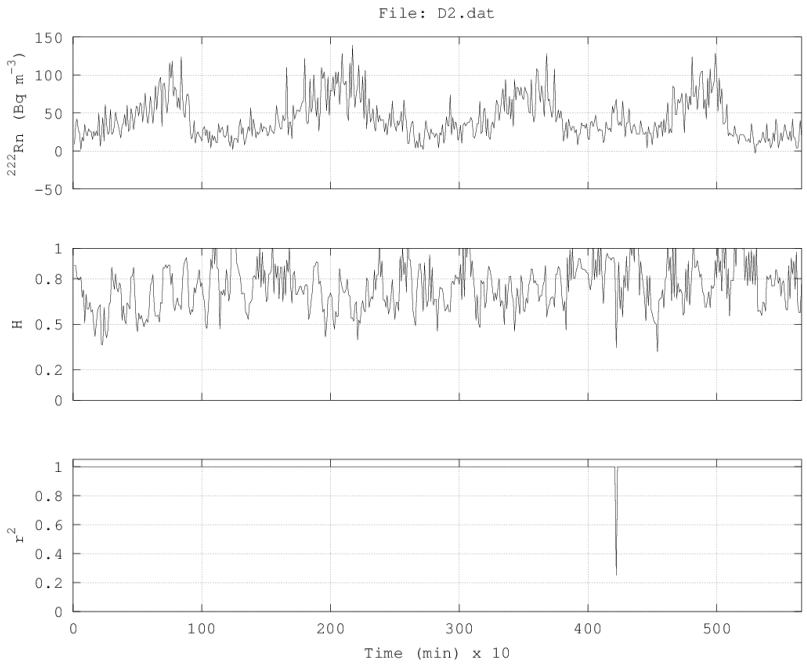

(a)

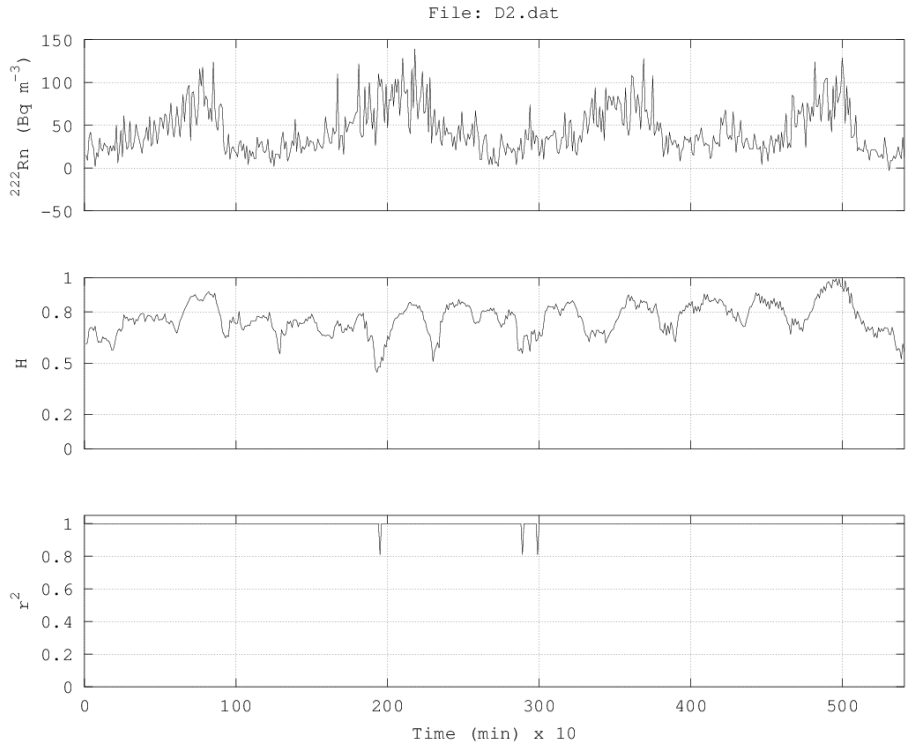

(b)

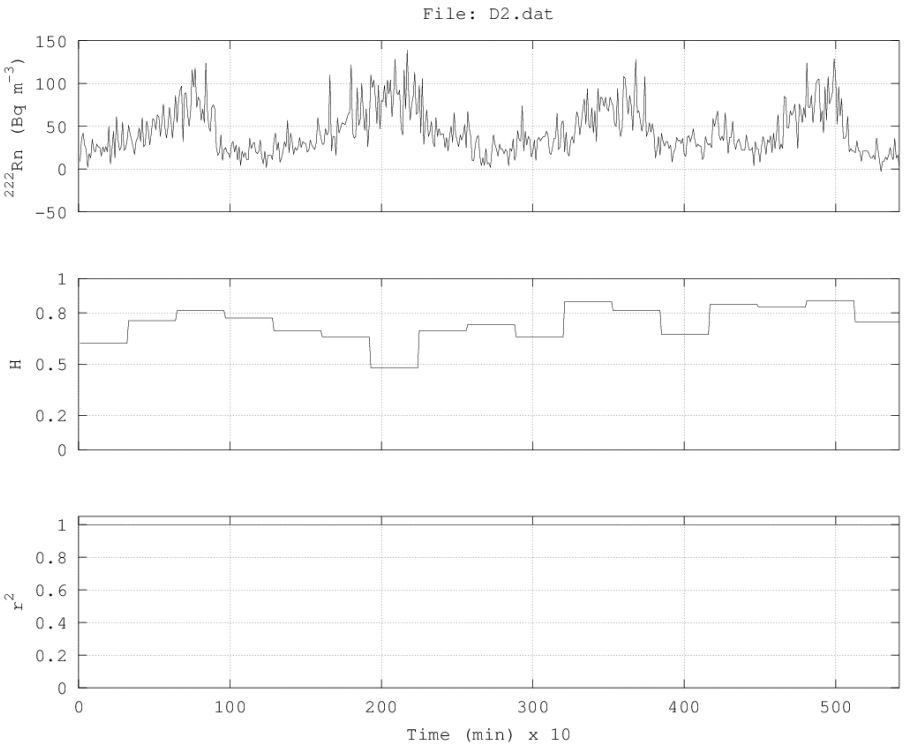

(c)

Figure 2: Radon concentrations and Hurst exponent evolution in dwelling D2. In all Figures, the top sub-Figure is the evolution of radon concentration, the middle sub-Figure is the evolution of Hurst exponent and the bottom sub-Figure is the evolution of the square of the linear correlation coefficient. R/S analysis: (a) sliding-window of length 8,step 1; (b) sliding-window of length 32,step 1; (c) lumping of window-length 32.

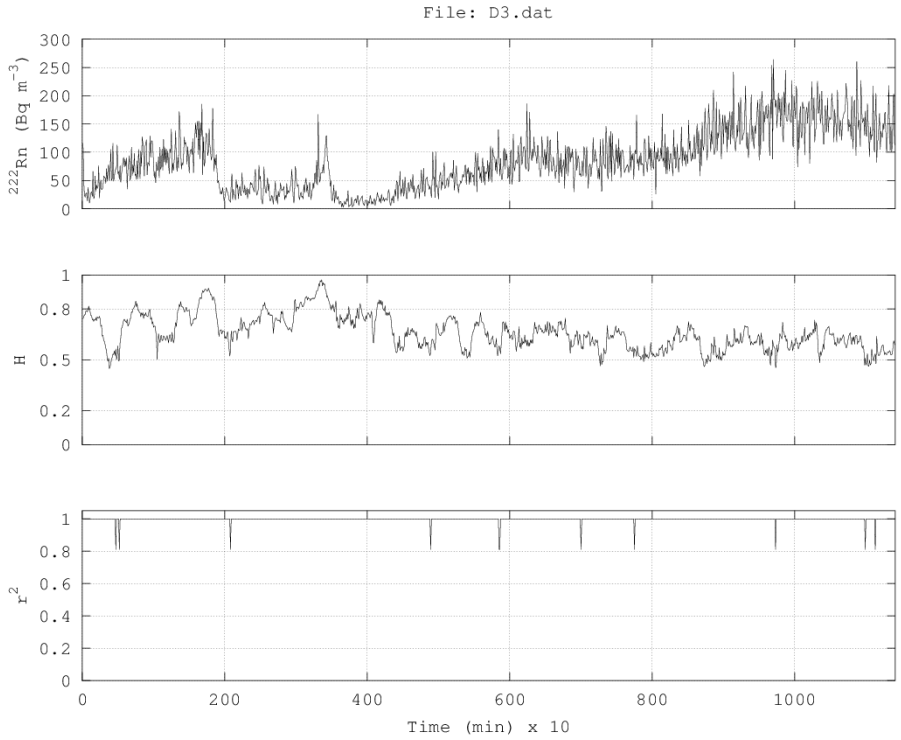

(a)

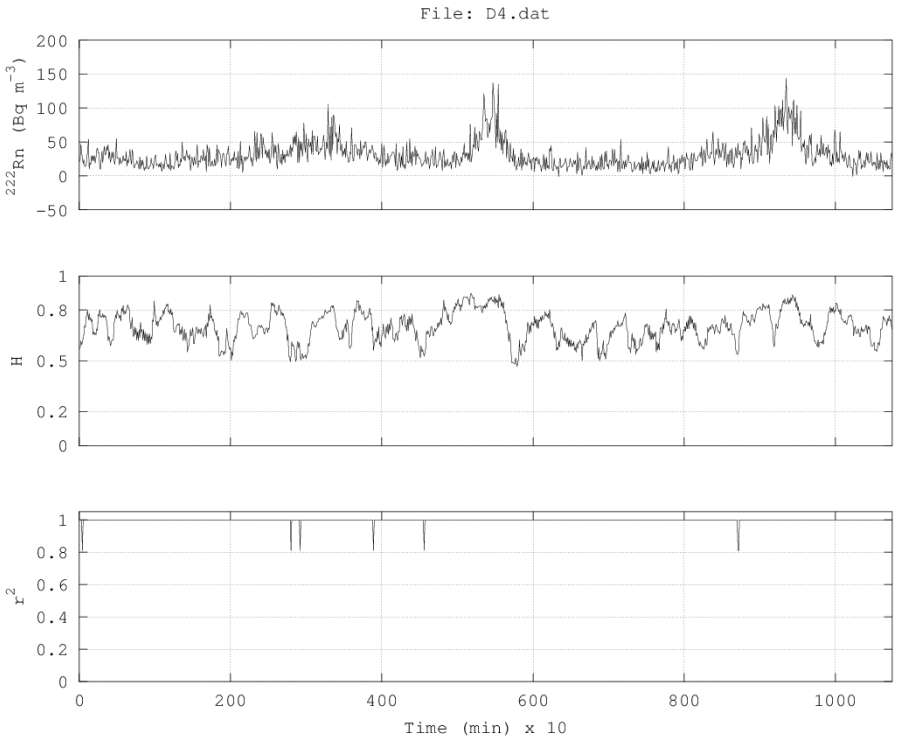

(b)

Figure 3: Radon concentrations and Hurst exponent evolution in dwellings D3 (a) and D4 (b). In all Figures, the top sub-Figure is the evolution of radon concentration, the middle sub-Figure is the evolution of Hurst exponent and the bottom sub-Figure is the evolution of the square of the linear correlation coefficient. R/S analysis of sliding-window of length 32.

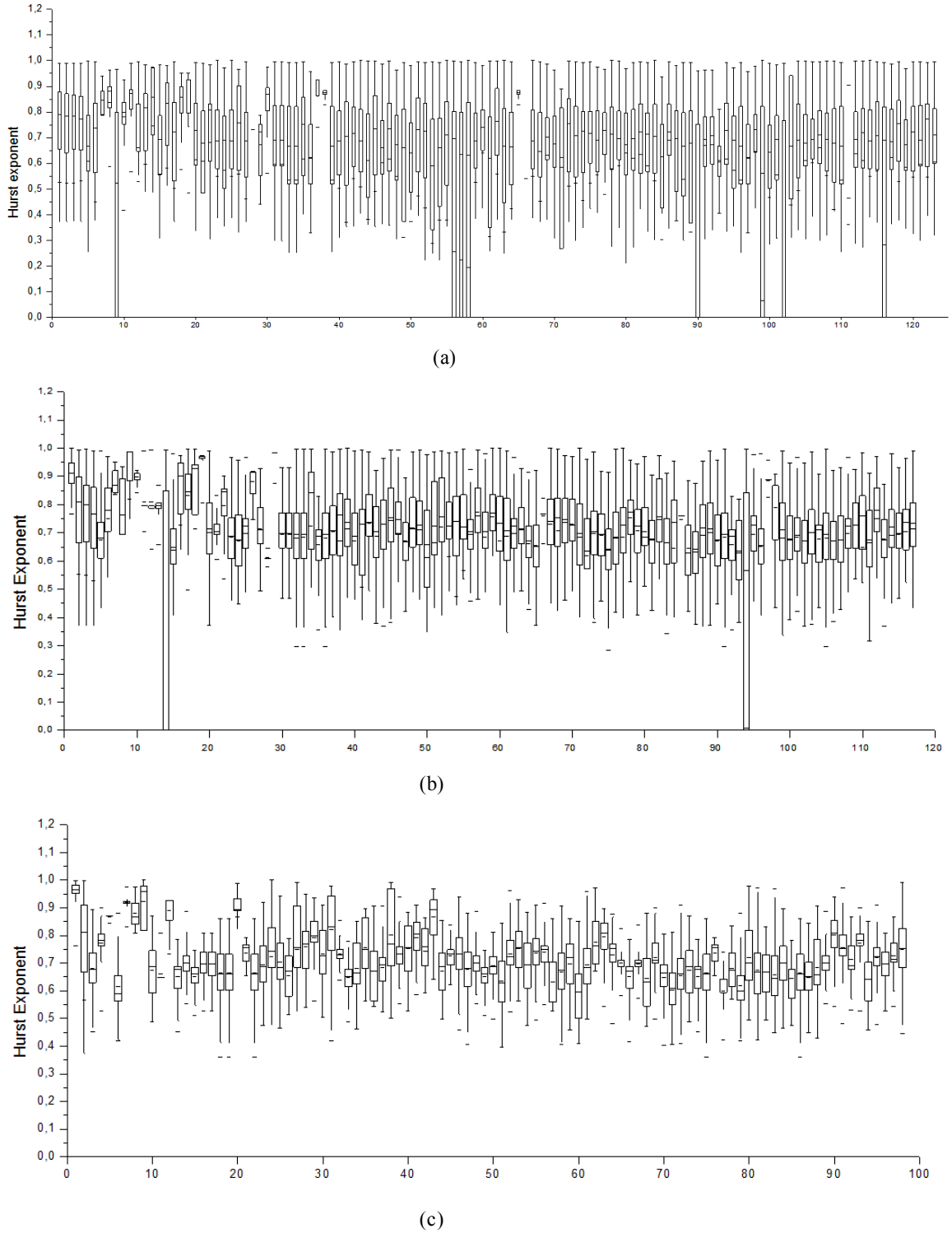

Figure 4: Box-whisker plots of Hurst exponent evolution outcomes in all investigated dwellings. Sliding-window R/S of step 1 and window-size (a) 8; (b) 16; (c) 32. The horizontal axis shows an identification number for each investigated dwelling.

window sizes, the main percentage of each box-whisker plot is within the region of persistency, i.e. H - values above 0.5. From another perspective, this implies that the majority of Hurst exponents indicate persistency, either with window size 8, 16 or 32. It is more important, that a vast number of segments exhibited H - values above 0.7 or even 0.8. These segments indicate strong persistency of the corresponding parts of the radon concentration signal. Note, however, that when small window sizes are employed in R/S analysis (size 8 or 16), some antipersistent areas of the signals are identified. As already implied, a window size of 8 corresponds only to 80 minutes of time-series of

indoor radon concentrations. This time duration is small enough to be biased by the several radon affecting factors. In this sense, the corresponding results just outline the signals' tendency in presenting persistent long-memory. They cannot evoke, in this consensus, emergence of any existing long-memory dynamics. These dynamics are emerged by the larger window size of 32. As also mentioned, this size is a good compromise between bias due to factors and smoothing due to radon peaking or downturn. It should be mentioned though that the 32-sample window-size rendered inconsistencies in some calculated Hurst exponents in twenty five radon time-series. For this reason, these series were excluded from the box-whisker plots of Figure3c.

Conclusion

Several dwellings were accessed and their indoor radon concentrations were measured with active techniques. Time-series of at-least one day duration were employed in this study. Utilizing R/S analysis through sliding window and lumping, numerous Hurst exponents were calculated for each useful time-series. The majority of exponents were found to be in the range of $0.5 < H < 1$ for the majority of the situations. This finding indicated persistency. Several exponents were above 0.8, namely the corresponding time-series parts were very persistent. In almost all cases it was found that indoor-radon dynamics are governed by chaos and long-memory.

Acknowledgements

This research has been co-financed by the European Union (European Social Fund-ESF) and Greek national funds through the Operational Program "Education and Lifelong Learning" of the National Strategic Reference Framework (NSRF)-Research Funding Program: THALES Investing in knowledge society through the European Social Fund.

References

1. Nazaroff W, Nero A (1988) Radon and its decay products in indoor air. Wiley, New York.
2. Appleton JD (2005) Radon in air and water. In: Selinus O, Alloway B, Centero J, Finkelman R, Fuge R, Lindh U, Smedley P (Eds.), Essentials of medical geology, impacts of the natural environment on public health. Elsevier Academic Press 227–262.
3. UNSCEAR (United Nations Scientific Committee on the Effects of Atomic Radiation) (2008) Sources and effects of ionizing radiation, UNSCEAR, New York.
4. Risica S (1998) Legislation on radon concentration at home and at work. Radiation Protection Dosimetry 78: 15–21.
5. Hu N, Zheng JF, Ding DX, Liu J, Yang LQ, et al. (2009) Metal pollution in Huayuan River in Hunan Province in China by manganese sulphate waste residue. Bull Environ Contam Toxicol 83: 583-590.
6. Ishikawa T, Narazaki Y, Yasuoka Y, Tokonami S, Yamada Y (2003) Bio-kinetics of radon ingested from drinking water. Radiat Prot Dosimetry 105: 65-70.
7. US-EPA (2000) United States-Environmental Protection Agency. Role on radionuclides in drinking water. 65 FR 76707 7 December 2000, EPA, New York.
8. EURATOM, European Commission (1990) Commission recommendation of the 21 Februay 1990 on the protection of the public against indoor exposure to radon. 390HO14390/143/EURATOM, L 080. 26-28.
9. Burkart W, Sohrabi M, Bayer A (2002) High levels of natural radiation and radon areas: radiation dose and health effects. Elsevier Science, Amsterdam 325.
10. Yu KN, Lau BM, Nikezic D (2006) Assessment of environmental radon hazard using human respiratory tract models. J Hazard Mater 132: 98-110.
11. Vogiannis E, Nikolopoulos D, Louizi A, Halvadakis CP (2004) Radon variations during treatment in thermal spas of Lesvos Island (Greece). Journal of Environmental Radioactivity 75:159-170.
12. Nikolopoulos D, Vogiannis E (2007) Modelling radon progeny concentration variations in thermal spas. Sci Total Environ 373: 82-93.
13. Bernhardt GP, Hess CT (1996) Acute exposure from 222Rn and aerosols in drinking water. Environment International 22: S753-S759.
14. Hurst H (1951) Long Term Storage Capacity of Reservoirs. Transactions of the American Society of Civil Engineers 116: 770-799.
15. Black R, Simaiki Y (1965) Long-term storage: an experimental study. Constable, London.
16. Lopez T, Martinez-Gonzalez C, Manjarrez J, Plascencia N, Balankin A (2009) Fractal Analysis of EEG Signals in the Brain of Epileptic Rats, with and without Biocompatible Implanted Neuroreservoirs. Applied Mechanics and Materials 15:127-136.
17. Dattatreya G (2005) Hurst Parameter Estimation from Noisy Observations of Data Traffic Traces. 4th WSEAS International Conference on Electronics, Control and Signal Processing, Miami, Florida, USA, 17-19 November, 193–198.
18. Gilmore M, Yu C, Rhodes T, Peebles W (2002) Investigation of rescaled range analysis, the Hurst exponent, and long-time correlations in plasma turbulence. Physics of Plasmas 9: 1312-1317.
19. Smirnova N, Hayakawa M, Gotoh K (2004) Precursory behavior of fractal characteristics of the ULF electromagnetic fields in seismic active zones before strong earthquakes. Physics and Chemistry of the Earth 29: 445–451.
20. Smirnova N, Hayakawa M (2007) Fractal characteristics of the ground-observed ULF emissions in relation to geomagnetic and seismic activities. Journal of Atmospheric and Solar-Terrestrial Physics 69: 1833–1841.
21. Rehman S, Siddiqi A (2009) Wavelet based Hurst exponent and fractal dimensional analysis of Saudi climatic dynamics. Chaos, Solitons and Fractals 39: 1081-1090.
22. Kilcik A, Anderson C, Rozelot J, Ye H, Sugihara G, Ozguc A (2009) Non linear prediction of solar cycle 24. The Astrophysical Journal 693: 1173–1177.
23. Granero MS, Segovia JT, Perez JG (2008) Some comments on Hurst exponent and the long memory processes on capital markets. Physica A 387: 5543–5551.
24. Eftaxias K, Kapiris P, Dologlou E, Kopanas J, Bogris N, et al. (2002) EM anomalies before the Kozani earthquake: a study of their behavior through laboratory experiments. Geophysical Research Letters 29: 69-1-69-4.
25. Eftaxias K, Kapiris P, Polygiannakis J, Bogris N, Kopanas J, et al. (2001) Signature of pending earthquake from electromagnetic anomalies. Geophysical Research Letters 29: 3321–3324.
26. Kapiris P, Polygiannakis J, Peratzakis A, Nomicos K, Eftaxias K (2002) VHF-electromagnetic evidence of the underlying pre-seismic critical stage. Earth Planets Space 54: 1237–1246.
27. Kapiris PG, Eftaxias KA, Nomikos KD, Polygiannakis J, Dologlou E, et al. (2003) Evolving towards a critical point: A possible electromagnetic way in which the critical regime is reached as the rupture approaches. Nonlinear Processes in Geophysics 10: 511–524.
28. Nikolopoulos D, Petraki E,Vogiannis E, Chaldeos Y, Yannakopoulos P, et al. (2013). Traces of self-organisation and long-range memory in variations of environmental radon in soil: Comparative results from monitoring in Lesvos Island and Ileia (Greece). Journal of Radioanaltical and Nuclear Chemistry 299: 203-219.
29. Nikolopoulos D, Louizi A, Koukouliou V, Serefoglou A, Georgiou E, et al. (2002) Radon survey in Greece--risk assesment. J Environ Radioact 63: 173-186.
30. Nikolopoulos D, Louizi A (2008) Study of indoor radon and radon in drinking water in Greece and Cyprus: Implications to exposure and dose. Radiation Measurements 43:1305-1314.
31. Karamanos K, Dakopoulos D, Aloupis K, Peratzakis A, Athanasopoulou L, et al. (2006) Preseismic electromagnetic signals in terms of complexity. Phys Rev E Stat Nonlin Soft Matter Phys 74: 016104.
32. Nikolopoulos D, Kottou S, Louizi A, Petraki E, Vogiannis E et al. (2014) Factors Affecting Indoor Radon Concentrations of Greek Dwellings through Multivariate Statistics - First Approach. J Phys Chem Biophys 4:145.